

Proton-Neutron Pairing Amplitude as a Generator Coordinate for Double-Beta Decay

Nobuo Hinohara^{1,2} and Jonathan Engel¹

¹*Department of Physics and Astronomy, University of North Carolina, Chapel Hill, North Carolina, 27599-3255, USA*

²*Center for Computational Sciences, University of Tsukuba, Tsukuba 305-8571, Japan*

We treat proton-neutron pairing amplitudes, in addition to the nuclear deformation, as generator coordinates in a calculation of the neutrinoless double-beta decay of ^{76}Ge . We work in two oscillator shells, with a Hamiltonian that includes separable terms in the quadrupole, spin-isospin, and pairing (isovector and isoscalar) channels. Our approach allows larger single-particle spaces than the shell model and includes the important physics of the proton-neutron quasiparticle random-phase approximation (QRPA) without instabilities near phase transitions. After comparing the results of a simplified calculation that neglects deformation with those of the QRPA, we present a more realistic calculation with both deformation and proton-neutron pairing amplitudes as generator coordinates. The future should see proton-neutron coordinates used together with energy-density functionals.

PACS numbers: 23.40.-s, 21.60.Jz, 24.10.Cn, 27.50.+e

Neutrinoless double-beta ($0\nu\beta\beta$) decay can occur only if neutrinos are Majorana particles. That fact has motivated many expensive and complicated experiments to search for the process. If it is observed, the decay can also reveal an overall neutrino mass scale, $m_\nu \equiv \sum_i U_{ei} m_i^2$ (where i labels the mass eigenstates, and U is the neutrino mixing matrix [1]), but only if we know the value of unobservable nuclear matrix elements that play a role in the decay. The entanglement of nuclear and neutrino physics has led nuclear-structure theorists to attempt to calculate the nuclear matrix elements. At present, various nuclear models agree to within factors of about three. More accurate calculations will increase the importance of both existing limits and any actual observation.

The method most often applied to double-beta decay is the proton-neutron (pn) quasiparticle random phase approximation (QRPA). QRPA calculations were the first to suggest that pn pairing quenches double-beta matrix elements [2, 3]. That result was surprising because evidence for such pairing in spectra and electromagnetic transitions or moments is hard to come by, particularly when the number of neutrons N is significantly larger than the number of protons Z , as it is in most nuclei that undergo double-beta decay. At the mean-field level, pn pairing never develops in those nuclei. But the QRPA uncovered pairing fluctuations that have significant effects on both single- and double-beta decay.

Despite this success, the QRPA is not fully realistic because it is built on small oscillations around a single mean field. That means that 1) it is not really suited for complicated but important double-beta-decay parents/daughters such as ^{76}Ge and ^{130}Xe , in which a single mean field provides a poor representation of the ground state, and 2) its predictions for the effects of pn pairing fluctuations, which are not small, cannot be fully trusted. To treat the physics more reliably, one needs a method in which collective pn pairing fluctuations are allowed to be large. One framework for large-amplitude modes is the generator-coordinate method (GCM) [4, 5], a variational procedure that works by mixing many mean-field wave functions with varying amounts of collectivity. To

treat large-amplitude quadrupole vibrations, for example, it produces a “collective wave function” that superposes Slater determinants (or generalizations) with different amounts of quadrupole deformation in an optimal way. In our work the pn pairing amplitude (defined below) will play the role of collective deformation.

In fact, a sophisticated version of the GCM, in conjunction with energy-density functional theory, has already been applied to double-beta decay [6–8]. The collective coordinates include only axial quadrupole deformation and particle-number fluctuation (from like-particle pairing), however, and so the calculations omit the suppression caused by pn pairing. Not surprisingly, the GCM results tend to be larger than those of e.g. the shell model, which includes pn pairing. If the pn pairing amplitude could be added as another coordinate in these GCM calculations, the matrix elements would probably shrink. No one has ever treated pn pairing as a GCM degree of freedom, however. Because pn pairing is less strongly collective than its like-particle counterpart, doing so requires a careful extension of mean-field methods and the GCM itself. In this paper we undertake that project and report a first application to the $0\nu\beta\beta$ decay of ^{76}Ge .

We begin with the matrix elements we wish to calculate. In the closure approximation (which is good to about 10% [9]), we can write the nuclear $0\nu\beta\beta$ matrix element in terms of the initial and final ground states and a two-body transition operator. If we neglect the “tensor term,” the effect of which is at most 10% [10, 11], and two-nucleon currents [12] (the effects of which are still uncertain) we can write the matrix element as

$$M^{0\nu} \equiv \langle F | \hat{M}_{0\nu} | I \rangle = \frac{2R}{\pi g_A^2} \int_0^\infty q dq \quad (1)$$

$$\times \langle F | \sum_{a,b} \frac{j_0(qr_{ab}) [h_F(q) + h_{GT}(q) \vec{\sigma}_a \cdot \vec{\sigma}_b]}{q + \bar{E} - (E_I + E_F)/2} \tau_a^+ \tau_b^+ | I \rangle,$$

where $|I\rangle$ and $|F\rangle$ are the ground states of the initial and final nuclei, r_{ab} is the distance between nucleons a and b , j_0 is the usual spherical Bessel function, and R is the

nuclear radius, inserted by convention to make the matrix element dimensionless. The form factors $h_F(q)$ and $h_{GT}(q)$ contain the vector and axial vector coupling constants, forbidden corrections to the weak current, nucleon form factors, and the “Argonne” short-range correlation function [13]. See, e.g., Ref. [14] for details; note that we absorb the inverse square of the axial-vector coupling constant into our definition of h_F .

To compute the matrix element in Eq. (1) we need good representations of the initial and final ground states $|I\rangle$ and $|F\rangle$. In this first application to $A = 76$ nuclei, we construct the states in a Hilbert space consisting of 36 particles moving freely in the oscillator fp and sdg shells. Our Hamiltonian has the form

$$H = h_0 - \sum_{\mu=-1}^1 g_{\mu}^{T=1} S_{\mu}^{\dagger} S_{\mu} - \frac{\chi}{2} \sum_{K=-2}^2 Q_{2K}^{\dagger} Q_{2K} - g^{T=0} \sum_{\nu=-1}^1 P_{\nu}^{\dagger} P_{\nu} + g_{ph} \sum_{\mu,\nu=-1}^1 F_{\nu}^{\mu\dagger} F_{\nu}^{\mu}, \quad (2)$$

where h_0 contains spherical single particle energies, Q_{2K} are the components of a quadrupole operator defined in Ref. [15], and

$$S_{\mu}^{\dagger} = \frac{1}{\sqrt{2}} \sum_l \hat{l} [c_l^{\dagger} c_l^{\dagger}]_{00\mu}^{001}, \quad P_{\mu}^{\dagger} = \frac{1}{\sqrt{2}} \sum_l \hat{l} [c_l^{\dagger} c_l^{\dagger}]_{0\mu 0}^{010}, \\ F_{\nu}^{\mu} = \frac{1}{2} \sum_i \sigma_i^{\mu} \tau_i^{\nu} = \sum_l \hat{l} [c_l^{\dagger} \bar{c}_l]_{0\mu\nu}^{011}. \quad (3)$$

In this last equation, c_l^{\dagger} is a creation operator, l labels single-particle multiplets with good orbital angular momentum, $\hat{l} \equiv \sqrt{2l+1}$, S_{μ}^{\dagger} creates a correlated isovector pair with orbital angular momentum $L = 0$ and spin $S = 0$ (and with μ labeling the isospin component T_z), P_{μ}^{\dagger} creates an isoscalar pn pair with $L = 0$ and $S = 1$ ($S_z = \mu$), and the F_{ν}^{μ} are the components of the Gamow-Teller operator. Although the Hamiltonian is not fully realistic, it combines and extends both the $SO(8)$ model [16, 17] and the pairing-plus-quadrupole model [15, 18], and contains the most important (collective) parts of shell-model interaction [19]. We discuss the values of the couplings in Eq. (2) shortly.

A direct diagonalization in a space this large is not possible, even with our simple Hamiltonian, and we have already discussed the drawbacks of the QRPA. We therefore turn to the GCM, which has been reviewed in many places (see, e.g., Ref. [4]) and is useful in very-large-scale shell-model problems. The procedure is variational, with an ansatz for the ground state of the form

$$|\Psi\rangle = \sum_{a_1 a_2 \dots a_n} f(a_1, a_2, \dots, a_n) \mathcal{P} |a_1, a_2, \dots, a_n\rangle. \quad (4)$$

Here the kets $|a_1, a_2, \dots, a_n\rangle$ are mean-field states — Slater determinants or, in our case, quasiparticle vacua — with n expectation values a_i specified, \mathcal{P} is an operator

that projects onto states with well-defined values for angular momentum and neutron and proton particle numbers, and f is a weight function. The starting point, if we want to include the effects of pn pairing, is a Hartree-Fock-Bogoliubov (HFB) code that mixes neutrons and protons in the quasiparticles, i.e. (schematically):

$$\alpha^{\dagger} \sim u_p c_p^{\dagger} + v_p c_p + u_n c_n^{\dagger} + v_n c_n. \quad (5)$$

The actual equations contain sums over single particle states as well, so that each of the u ’s and v ’s above are replaced by matrices as described, e.g., in Ref. [20].

We use the generalized HFB (neglecting the Fock terms in this step) without any symmetry restriction to construct a set of quasiparticle vacua that are constrained to have a particular deformation β (defined here as $0.438 \text{ fm}^2 \text{ MeV}^{-1} \chi \langle Q_{20} \rangle$) and isoscalar-pairing amplitude $\phi = \langle P_0 + P_0^{\dagger} \rangle / 2$ (these are the a_i in Eq. (4)), that is, we solve the HFB equations for the Hamiltonian with linear constraints

$$H' = H - \lambda_Z N_Z - \lambda_N N_N - \lambda_Q Q_{20} - \frac{\lambda_P}{2} (P_0 + P_0^{\dagger}), \quad (6)$$

where the N_Z and N_N are the proton and neutron number operators — they are part of the usual HFB minimization — and the other λ ’s are Lagrange multipliers to fix the deformation and isoscalar pairing amplitude. (When computing the Fermi part of the $0\nu\beta\beta$ matrix element we substitute the isovector pn operators $(S_0 - S_0^{\dagger})/2i$ for $(P_0 + P_0^{\dagger})/2$ in Eq. (6).) As already noted, without the last multiplier the isoscalar pairing amplitude vanishes unless the strength $g^{T=0}$ of the corresponding interaction is larger than some critical value. For realistic Hamiltonians that is never the case, hence the need to generate amplitudes by force, as it were.

Having obtained a set of HFB vacua with varying amounts of axially symmetric deformation and pn pairing, we project the vacua onto states with the correct number of neutrons and protons and with angular momentum zero. We then solve the Hill-Wheeler equation [4], which amounts to diagonalizing H in the space spanned by our nonorthogonal projected vacua, to determine the weight function f in Eq. (4).

To carry out a fairly realistic calculation, we need appropriate values for the couplings in the Hamiltonian of Eq. (2). We determine them by trying to reproduce the results of calculations with two different Skyrme interactions (SkO’ [21] and SkM* [22]) in ^{76}Ge and neighboring nuclei. We first do Skyrme-HFB calculations [23] in ^{76}Ge to determine appropriate volume pairing constants. We then take single-particle energies for each nucleus, which we show for SkO’ in Table I, from the results of constrained HFB calculations for ^{76}Ge and ^{76}Se , which we temporarily force to be spherical. Next we adjust the like-particle part of our isovector pairing interaction ($g_1^{T=1}$ and $g_{-1}^{T=1}$) to get the same pairing gaps as the original Skyrme calculations. The resulting occupation numbers are close to the spherical Skyrme-HFB numbers

TABLE I. Neutron and proton canonical single-particle energies (in MeV) taken from spherical HFB with SkO'.

	^{76}Ge (n)	^{76}Ge (p)	^{76}Se (n)	^{76}Se (p)
p1/2	-10.31	-6.80	-11.21	-5.06
p3/2	-12.69	-9.56	-13.72	-7.81
f5/2	-9.94	-7.47	-11.08	-5.61
f7/2	-17.63	-15.90	-18.87	-13.95
s1/2	-0.49	6.27	-0.90	7.05
d3/2	1.49	7.94	1.17	8.77
d5/2	-2.60	2.64	-3.26	3.65
g7/2	3.23	6.43	2.24	8.08
g9/2	-8.09	-6.31	-9.31	-4.46

(and, as is typical for such calculations, relatively different from the measured occupations of Refs. [24, 25]). The Coulomb interaction is not included explicitly in our Hamiltonian, but its effects are present in single-particle energies and the fit isovector pairing interaction.

Next, we fix our quadrupole interaction so that it reproduces the prolate deformation of Skyrme-HFB calculations, now with axial deformation allowed, in ^{76}Ge and ^{76}Se . The top panel of Fig. 1 compares the diagonal part of the Hamiltonian kernel $\langle \beta, \phi = 0 | H | \beta, \phi = 0 \rangle$ as a function of β (we refer this function as a potential energy surface) in the Skyrme HFB and in our model. The lowest minima are prolate in both nuclei. In ^{76}Se the surfaces have oblate minima around $\beta = -0.2$ as well, but in general the surfaces are quite flat. (We discuss the bottom part of the figure later.)

Turning to the particle-hole spin-isospin interaction, we take g_{ph} from a deformed Skyrme-QRPA calculation [26], with the relevant piece of the time-odd functional adjusted as in Ref. [27] to put the Gamow-Teller resonance in ^{76}Ge at the correct energy. The resulting values of g_{ph} , extracted as in Ref. [28], are $1.9 \times \bar{g}^{T=1}$ for SkO' and $0.9 \times \bar{g}^{T=1}$ for SkM*, where $\bar{g}^{T=1}$ is the average of the two like-particle pairing strengths. To fix the pn part of our $T = 1$ pairing interaction, we adjust $g_0^{T=1}$ to make two-neutrino Fermi decay vanish (in the closure approximation); this last step approximates isospin restoration [29]. We find $g_0^{T=1} = 1.05 \times \bar{g}^{T=1}$ for SkO' and $0.98 \times \bar{g}^{T=1}$, for SkM*.

That then leaves just the crucial isoscalar pairing strength, $g^{T=0}$. There is no consensus about how best to determine that parameter. We do so by fitting the measured total β^+ strength $B(\text{GT}+)$ from ^{76}Se as well as possible. Two separate charge-exchange experiments [30, 31] have tried to extract $B(\text{GT}+)$. Neither isolates the quantity perfectly but both are consistent with the assumption that $B(\text{GT}+) \approx 1$, and we adopt that value. It is not obvious how much the experimental strength is quenched by states outside the model space, so we always do two fits, one (unquenched) as just described and one (quenched) in which we scale our calculated strength by

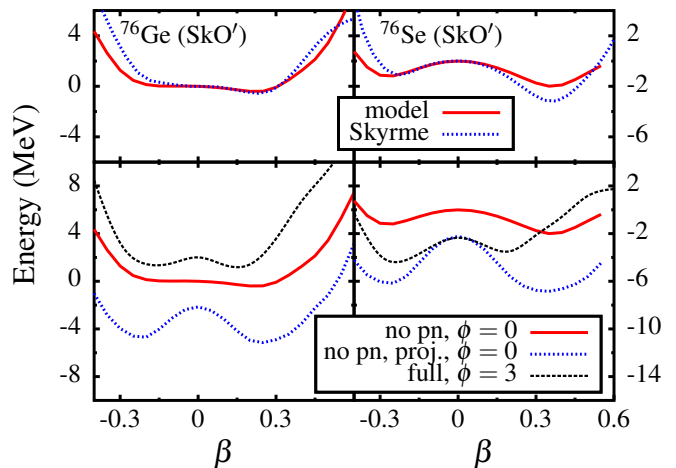


FIG. 1. (Color online.) **Upper panels:** Potential energy surfaces for SkO' (dotted line) and our corresponding model interaction (solid line) at $\phi = 0$ with no spin-isospin or isoscalar pairing interactions (together denoted by “ pn ” in the lower panels) as functions of β for ^{76}Ge (left) and ^{76}Se (right). **Lower panels:** Potential energy surface from the model without projection and pn at $\phi = 0$ (solid red line, same line as in upper figure), with projection but still without pn at $\phi = 0$ (dotted blue line), and with both projection and pn at $\phi = 3$ (dashed black line). Energy is measured from the unprojected value at $\beta = 0$.

$$(1/1.27)^2 = 0.62.$$

Of course, the value we extract for $g^{T=0}$ will depend on our choice of generator coordinates as well as assumptions about quenching. Before turning to the full calculation outlined above we discuss a simpler and more transparent case, in which the quadrupole force is turned off and the isoscalar pairing amplitude (or isovector pn pairing amplitude when we calculate the Fermi matrix element) is the sole coordinate. Though the isoscalar pairs create a spin vector that always breaks rotational symmetry and forces us to do angular-momentum projection, the absence of a quadrupole force makes both the initial and final nuclear densities nearly spherical. The main advantage of spatial spherical symmetry is that we can compare the results with those of the spherical QRPA, for which we developed a code.

With a single generator coordinate and the interaction we extract from SkO' (minus the quadrupole part), there is no value of $g^{T=0}$ for which $B(\text{GT}+)$ from ^{76}Se is as small as 1, much less 0.62; we therefore let $g^{T=0} = 1.47 \times \bar{g}^{T=1}$, the value for which $B(\text{GT}+)$ is the smallest. With the interaction we extract from SkM*, whether we quench our strength or not, there are two values of $g^{T=0}$ that produce the correct β^+ strength — 0.82 and 1.56 (unquenched) or 0.33 and 1.77 (quenched), all in units of $\bar{g}^{T=1}$ — and we choose the larger value in each case. With all parameters finally determined, we can calculate the $0\nu\beta\beta$ matrix element; Table II displays the results at various stages of approximation.

In our QRPA calculation, we adjust $g^{T=0}$ (commonly

TABLE II. The $0\nu\beta\beta$ matrix element $M^{0\nu}$ for the decay of ^{76}Ge in a simplified calculation that neglects deformation, at various levels of approximation. The first column contains the source of the couplings in Eq. (2), the second the matrix element when the spin-isospin and isoscalar pairing interactions are absent, the third the matrix element with only isoscalar pairing missing, the fourth the full GCM result, and the last the result of the QRPA with the same Hamiltonian (except for a slightly modified $g^{T=0}$). The matrix elements in parentheses are obtained by quenching our $B(\text{GT}+)$.

Skyme	no $g_{ph}, g^{T=0}$	no $g^{T=0}$	full	QRPA
SkO'	14.0	9.5	5.4 (5.4)	5.6 (5.0)
SkM*	11.8	9.4	4.1 (2.8)	3.5 (2.5)

called g_{pp} when divided by $\bar{g}^{T=1}$) in exactly the same way. The values we obtain are only slightly different. The last column of Table II contains the QRPA $0\nu\beta\beta$ matrix elements. They are fairly close to those of the GCM calculation, but much more sensitive to $g^{T=0}$.

To clarify this last statement, we show the GCM and QRPA matrix elements as functions of $g^{T=0}/\bar{g}^{T=1}$ in Fig. 2. The QRPA curves lie slightly above their GCM counterparts until $g^{T=0}/\bar{g}^{T=1}$ reaches a critical value slightly larger than 1.5; at that point a mean-field phase transition from an isovector pair condensate to an isoscalar condensate causes the famous QRPA “collapse.” The collapse is spurious, as the GCM results show. Its presence in mean-field theory makes the QRPA unreliable near the critical point. It is actually a bit of a coincidence that the QRPA matrix elements in the table are as close as they are to those of the GCM; a small change in $g^{T=0}$ would affect them substantially (though because it also alters $B(\text{GT}+)$ a lot, fitting to $B(\text{GT}+) = 0.62$ rather than 1.0 does not have a huge effect on the $0\nu\beta\beta$ matrix element). The GCM result is not only better behaved near the critical point but also, we believe, quite accurate. In the $SO(8)$ model used to test many-body methods in $\beta\beta$ decay many times, the GCM result is nearly exact for all $g^{T=0}$. That is not the case for extensions of the QRPA that attempt to ameliorate its shortcomings [32, 33], though some of those work better around the phase transition than others.

To show why the GCM behaves well, we display in the bottom right part of Fig. 3 the quantity $\mathcal{N}_{\phi_I}\mathcal{N}_{\phi_F}\langle\phi_F|\mathcal{P}_F\hat{M}_{0\nu}\mathcal{P}_I|\phi_I\rangle$, where $|\phi_I\rangle$ is a quasiparticle vacuum in ^{76}Ge constrained to have isoscalar pairing amplitude ϕ_I , ϕ_F is an analogous state in ^{76}Se , \mathcal{P}_I , \mathcal{P}_F project onto states with angular momentum zero and the appropriate values of Z and N , and $\mathcal{N}_{\phi_I}, \mathcal{N}_{\phi_F}$ normalize the projected states. This quantity is the contribution to the $0\nu\beta\beta$ matrix element from states with particular values of the initial and final isoscalar pairing amplitudes. The contribution is positive around zero condensation in the two nuclei and negative when the final pairing amplitude is large. Thus the GCM states must contain components with significant pn pairing when $g^{T=0}$ is near its fit

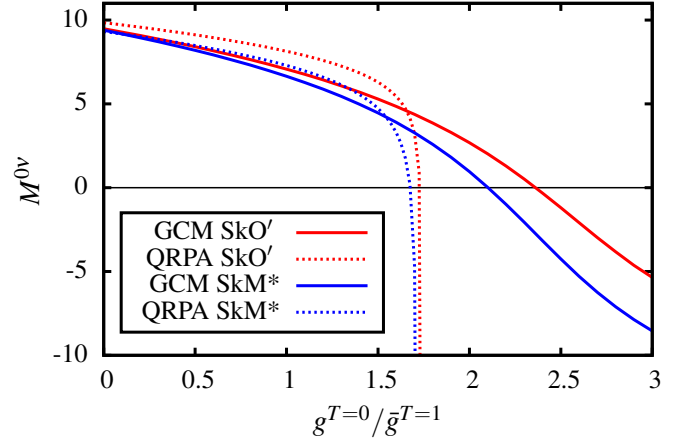


FIG. 2. (Color online.) Dependence of the GCM (solid) and QRPA (dashed) $0\nu\beta\beta$ matrix elements on the strength $g^{T=0}$ of the isoscalar pairing interaction. The red (upper) and blue (lower) lines of each type correspond to the interaction parameters extracted from SkO' and SkM*. The divergence in the QRPA near $g^{T=0}/\bar{g}^{T=1} = 1.5$ is discussed in the text.

value. The appearance of this plot is different from those in which the matrix element is plotted versus initial and final deformation [6–8]. Here the matrix element is small or negative even if the initial and final pairing amplitudes have the same value, as long as that value is large. The behavior reflects the qualitatively different effects of isovector and isoscalar pairs on the matrix element [3], effects that have no analog in the realm of deformation.

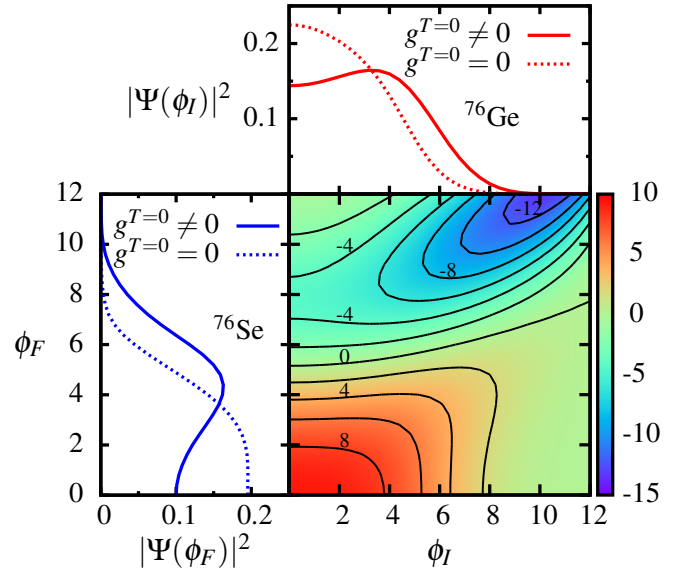


FIG. 3. (Color online.) **Bottom right:** $\mathcal{N}_{\phi_I}\mathcal{N}_{\phi_F}\langle\phi_F|\mathcal{P}_F\hat{M}_{0\nu}\mathcal{P}_I|\phi_I\rangle$ for projected quasiparticle vacua with different values of the initial and final isoscalar pairing amplitudes ϕ_I and ϕ_F , from the SkO'-based interaction (see text). **Top and bottom left:** Square of collective wave functions in ^{76}Ge and ^{76}Se .

The weight function f in the GCM ansatz multiplies non-orthogonal states and so is not really a “collective ground-state wave function.” The object that does play that role for is a member of an orthogonalized set defined, e.g., in Refs. [4] and [7]. The top and left parts of Fig. 3 show the square of this collective wave function for ^{76}Ge and ^{76}Se , with $g^{T=0}$ set both to zero and the fit value. It is clear in both nuclei, but particularly in ^{76}Se , that the isoscalar pairing interaction pushes the wave function into regions of large ϕ , where the matrix element in the bottom right panel is significantly reduced. It is also clear that for $g^{T=0} \neq 0$ the collective wave functions are far from the Gaussians that one would obtain in the harmonic (QRPA) approximation. Isoscalar pairing really is, and must be treated as, a large-amplitude mode.

We turn finally to the more realistic calculation that includes both deformation and the pn pairing amplitude as generator coordinates. We fit the couplings in H just as described earlier; the strength of the quadrupole interaction no longer vanishes and some of the other parameters change slightly: $g_0^{T=1} = 0.90$ for the interaction based on SkO' and 0.79 for that based on SkM*, and $g^{T=0} = 1.75$ for SkO' and 1.51 for SkM*, in units of $\bar{g}^{T=1}$. The calculated $B(\text{GT}+)$ in both cases is larger than the experimental data with or without quenching, which therefore does not alter the value of $g^{T=0}$.

First we analyze the influence of the number and angular-momentum projection on energy. The bottom part of Fig. 1 shows the projected potential energy surfaces $\langle \beta, \phi | \mathcal{P} H \mathcal{P} | \beta, \phi \rangle$ for two values of ϕ , along with the unprojected surface from the top part of the panel. Projecting at $\phi = 0$ without including pn interactions, the figure shows, lowers the energy by several MeV. The correlation energy from the angular momentum projection is large in the deformed regions, and projection causes both the oblate and prolate configurations that are low lying before projection to become clear minima.

With the pn interactions included, we present the surface at $\phi = 3$, where the collective wave function peaks, rather than at $\phi = 0$. The curve is shifted up by the repulsive spin-isospin interaction and downward by the isoscalar pairing, so that the final location depends on the relative sizes of g_{ph} and $g^{T=0}$. The SkO'-based interaction has a particularly large g_{ph} and so the final curve is higher than the initial unprojected curve without the pn terms. The curves flatten and in ^{76}Se the oblate minimum becomes the lowest.

Table III shows the GCM correlation energies themselves with successively more pn interaction included. The spin-isospin term in the Hamiltonian increases the energies by about 15 MeV for the SkO'-based interaction, which again, is quite strong in that channel, and 8 MeV for the SkM*-based interaction. The isoscalar pairing interaction then decreases the energy by 10–13 MeV, depending on the nucleus and interaction.

Finally, Fig. 4 shows the squares of the collective wave functions in β and ϕ . These wave functions closely mirror the projected potential energy surfaces. As in the

TABLE III. GCM ground state energies, in MeV, with both deformation and isoscalar pairing as generator coordinates. The energies are measured from the energy of the state with $\beta = 0$, $\phi = 0$, $g_{ph} = g^{T=0} = 0$ and no projection.

	SkO'		SkM*	
	^{76}Ge	^{76}Se	^{76}Ge	^{76}Se
no $g_{ph}, g^{T=0}$	-6.0	-8.1	-5.5	-7.1
no $g^{T=0}$	+10.5	+6.6	+2.1	-0.9
full	-0.9	-6.9	-7.7	-12.4

example without deformation, the peaks are at nonzero isoscalar-pairing amplitude. Regarding deformation, the largest peak is in the prolate region for ^{76}Ge and in the oblate region for ^{76}Se . Though that is also the case in the calculations of Refs. [6–8], our wave functions are still quite different from the ones in those papers, and our matrix element is less suppressed. The full result of our calculation is $M^{0\nu} = 4.7$, with both the SkO'- and SkM*-based interactions. The number breaks down into 3.4 from the Gamow-Teller operator and 1.2 from the Fermi operator for SkO', and 3.7 from the Gamow-Teller operator and 1.0 from the Fermi operator for SkM*.

In summary, the ease with which the GCM works in a large model space, even with several coordinates, means that it can include physics that is beyond the shell model. And because it mixes mean fields and has no issues with phase transitions, it offers a more comprehensive and accurate treatment of correlations than does the QRPA. One direction for future research in the pn GCM is a more complete effective interaction in multi-shell model spaces; another, perhaps more important, is an implementation together with Skyrme and Gogny energy-density functionals or with their successors. The combination of projection and GCM with density-functional theory poses a few conceptual problems (see, e.g., Ref. [34]) but recent progress suggests that they will be resolved before too long. The inclusion of pn degrees of freedom as generator coordinates should soon improve the quality of density-functional-based double-beta matrix elements.

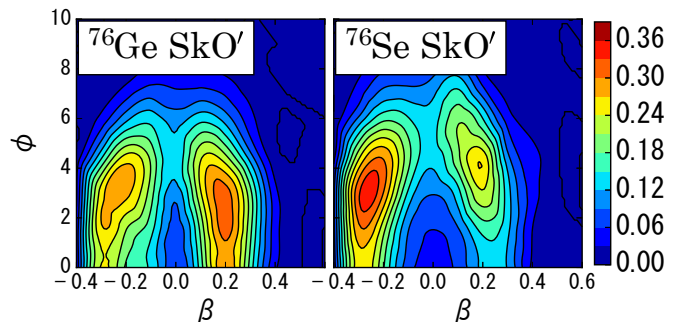


FIG. 4. (Color online.) Square of the collective wave functions in the calculation that includes deformation, in ^{76}Ge (left) and ^{76}Se (right), for the SkO'-based interaction.

We gratefully acknowledge useful discussions with T. R. Rodríguez. This work was supported by the U.S. Department of Energy through Contract No. DE-FG02-97ER41019, and JUSTIPEN (Japan-U.S. Theory Insti-

tute for Physics with Exotic Nuclei) under Grant No. DE-FG02-06ER41407 (U. Tennessee). We used computational resources at the National Institute for Computational Sciences (<http://www.nics.tennessee.edu/>).

-
- [1] F. T. Avignone III, S. R. Elliott, and J. Engel, *Rev. Mod. Phys.* **80**, 481 (2008).
 - [2] P. Vogel and M. R. Zirnbauer, *Phys. Rev. Lett.* **57**, 3148 (1986).
 - [3] J. Engel, P. Vogel, and M. R. Zirnbauer, *Phys. Rev. C* **37**, 731 (1988).
 - [4] P. Ring and P. Schuck, *The Nuclear Many-Body Problem*, Texts and Monographs in Physics (Springer, 2004).
 - [5] M. Bender, P.-H. Heenen, and P.-G. Reinhard, *Rev. Mod. Phys.* **75**, 121 (2003).
 - [6] T. R. Rodríguez and G. Martínez-Pinedo, *Phys. Rev. Lett.* **105**, 252503 (2010).
 - [7] T. R. Rodríguez and G. Martínez-Pinedo, *Prog. Part. Nucl. Phys.* **66**, 436 (2011).
 - [8] N. L. Vaquero, T. R. Rodríguez, and J. L. Egido, *Phys. Rev. Lett.* **111**, 142501 (2013).
 - [9] G. Pantis and J. Vergados, *Phys. Lett. B* **242**, 1 (1990).
 - [10] M. Kortelainen and J. Suhonen, *Phys. Rev. C* **75**, 051303(R) (2007).
 - [11] J. Menéndez, A. Poves, E. Caurier, and F. Nowacki, *Nucl. Phys. A* **818**, 139 (2009).
 - [12] J. Menéndez, D. Gazit, and A. Schwenk, *Phys. Rev. Lett.* **107**, 062501 (2011).
 - [13] F. Šimkovic, A. Faessler, H. Mütter, V. Rodin, and M. Stauf, *Phys. Rev. C* **79**, 055501 (2009).
 - [14] F. Šimkovic, A. Faessler, V. Rodin, P. Vogel, and J. Engel, *Phys. Rev. C* **77**, 045503 (2008).
 - [15] M. Baranger and K. Kumar, *Nucl. Phys. A* **110**, 490 (1968).
 - [16] J. Engel, S. Pittel, M. Stoitsov, P. Vogel, and J. Dukelsky, *Phys. Rev. C* **55**, 1781 (1997).
 - [17] G. Dussel, E. Maqueda, R. Perazzo, and J. Evans, *Nucl. Phys. A* **460**, 164 (1986).
 - [18] L. S. Kisslinger and R. A. Sorensen, *Rev. Mod. Phys.* **35**, 853 (1963).
 - [19] M. Dufour and A. P. Zuker, *Phys. Rev. C* **54**, 1641 (1996).
 - [20] A. L. Goodman, *Advances in Nuclear Physics*, edited by J. V. Negele and E. Vogt, Vol. 11 (Plenum Press, New York, 1979) p. 263.
 - [21] P.-G. Reinhard, D. J. Dean, W. Nazarewicz, J. Dobaczewski, J. A. Maruhn, and M. R. Strayer, *Phys. Rev. C* **60**, 014316 (1999).
 - [22] J. Bartel, P. Quentin, M. Brack, C. Guet, and H.-B. Håkansson, *Nucl. Phys. A* **386**, 79 (1982).
 - [23] M. Stoitsov, N. Schunck, M. Kortelainen, N. Michel, H. Nam, E. Olsen, J. Sarich, and S. Wild, *Comput. Phys. Commun.* **184**, 1592 (2013).
 - [24] J. P. Schiffer, S. J. Freeman, J. A. Clark, C. Deibel, C. R. Fitzpatrick, S. Gros, A. Heinz, D. Hirata, C. L. Jiang, B. P. Kay, A. Parikh, P. D. Parker, K. E. Rehm, A. C. C. Villari, V. Werner, and C. Wrede, *Phys. Rev. Lett.* **100**, 112501 (2008).
 - [25] B. P. Kay, J. P. Schiffer, S. J. Freeman, T. Adachi, J. A. Clark, C. M. Deibel, H. Fujita, Y. Fujita, P. Grabmayr, K. Hatanaka, D. Ishikawa, H. Matsubara, Y. Meada, H. Okamura, K. E. Rehm, Y. Sakemi, Y. Shimizu, H. Shimoda, K. Suda, Y. Tameshige, A. Tamii, and C. Wrede, *Phys. Rev. C* **79**, 021301 (R) (2009).
 - [26] M. T. Mustonen, T. Shafer, Z. Zenginerler, and J. Engel, *Phys. Rev. C* **90**, 024308 (2014).
 - [27] M. Bender, J. Dobaczewski, J. Engel, and W. Nazarewicz, *Phys. Rev. C* **65**, 054322 (2002).
 - [28] P. Sarriguren, E. M. de Guerra, A. Escuderos, and A. C. Carrizo, *Nucl. Phys. A* **635**, 55 (1998).
 - [29] F. Šimkovic, V. Rodin, A. Faessler, and P. Vogel, *Phys. Rev. C* **87**, 045501 (2013).
 - [30] R. L. Helmer, M. A. Punyasena, R. Abegg, W. P. Alford, A. Celler, S. El-Kateb, J. Engel, D. Frekers, R. S. Henderson, K. P. Jackson, S. Long, C. A. Miller, W. C. Olsen, B. M. Spicer, A. Trudel, and M. C. Vetterli, *Phys. Rev. C* **55**, 2802 (1997).
 - [31] E.-W. Grewe, C. Bäumler, H. Dohmann, D. Frekers, M. N. Harakeh, S. Hollstein, H. Johansson, L. Popescu, S. Rakers, D. Savran, H. Simon, J. H. Thies, A. M. van den Berg, H. J. Wörtche, and A. Zilges, *Phys. Rev. C* **78**, 044301 (2008).
 - [32] J. Toivanen and J. Suhonen, *Phys. Rev. Lett.* **75**, 410 (1995).
 - [33] V. Rodin and A. Faessler, *Phys. Rev. C* **66**, 051303 (2002).
 - [34] M. Bender, T. Duguet, P.-H. Heenen, and D. Lacroix, *Int. J. Mod. Phys. E* **20**, 259 (2011).